



# **iJRASET**

International Journal For Research in  
Applied Science and Engineering Technology



---

# **INTERNATIONAL JOURNAL FOR RESEARCH**

IN APPLIED SCIENCE & ENGINEERING TECHNOLOGY

---

**Volume: 11    Issue: 1    Month of publication: January 2023**

**DOI: <https://doi.org/10.22214/ijraset.2023.48866>**

**[www.ijraset.com](http://www.ijraset.com)**

**Call:  08813907089**

**E-mail ID: [ijraset@gmail.com](mailto:ijraset@gmail.com)**

# Non-Linear Peristaltic Flow of Power-Law Fluid in the Tapered Asymmetric Channel

J. Kamalakkannan<sup>1</sup>, C. Dhanapal<sup>2</sup>, M. Kothandapani<sup>3</sup>

<sup>1</sup>Research Scholar, Research and Development Center, Bharathiar University, Coimbatore 641046, Tamilnadu, India

<sup>2</sup>Department of Science and Humanities, Adhiparasakthi College of Engineering, Kalavai 632506, Tamilnadu, India

<sup>3</sup>Department of Mathematics, University College of Engineering, Arni, Tamil Nadu 632326, Tamilnadu, India

**Abstract:** *The effect of non-uniform wall properties on the peristaltic flow of a power law fluid in an asymmetric channel is investigated under Long wavelength and low Reynolds number assumptions. The tapered channel asymmetry is produced by choosing the peristaltic wave train on non-uniform walls to have different amplitudes and phase. Exact solutions are established for the longitudinal velocity, stream function, and pressure gradient. The expression for an average rise in pressure is computed numerically by evaluating the numerical integration. The effect of the power-law nature of the fluid on trapping is studied in detail. Prominent features of the key parameters entering the present flow are also displayed, and important conclusions are pointed out.*

**Keywords:** *Peristaltic flow; power-law fluid; tapered asymmetric channel.*

## I. INTRODUCTION

The problem of peristaltic motion has grown with more attention in recent times and in the past few years there have been diverse explorations [1-12] which deal with theoretical and experimental aspects of peristaltic motion of Newtonian fluids and non – Newtonian fluids. Because peristalsis is encountered in numerous physiological flows, a truthful mathematical study can help the major contributing factors to many flows in the human body. Such a motion is common in physiological flows, particularly in the ureters, intestines and arterioles. In fact, the peristaltic pressure distribution inside the ureters measured as a function of time is one of the important diagnostic tools in urology. In these cases roving sinusoidal waves in the wall of a vessel propels the fluid beside the tube. Within firm limits it is possible to pump peristaltically adjacent to a pressure gradient.

Many authors investigated blood and other bio-fluids to behave like a Newtonian fluid for physiological peristalsis. Although this approach offers a satisfactory understanding of peristalsis mechanism in ureter, it fails to give an enhanced understanding when the peristaltic mechanism is concerned in small blood vessels, lymphatic vessels and intestine. It is now established that most of the bio-fluids perform like non-Newtonian fluids [13-17]. Raju and Devanathan [18] have first premeditated the peristaltic transport of power-law fluid and they have achieved the stream function as a perturbation series in the amplitude ratio. Radahakrishnamacharya [19] considered the peristaltic motion of a power-law fluid under long wave length approximation. Shukla and Gupta [20] studied the peristaltic transport of a power-law fluid with variable viscosity. Srivastava and Srivastava [21] deliberated the peristaltic transport of a power-law fluid in uniform and non-uniform two dimensional channels.

Some of the physiological systems cannot be studied by a symmetric channel, especially the sagittal cross section of the uterus. Eytan and Elad [22] and Eytan et al. [23] have examined the intra uterine fluid flow in the sagittal cross section of the uterus by an asymmetric channel under lubrication approach. Subba Reddy et al. [24] have studied the Peristaltic motion of a power-law fluid in an asymmetric channel. Using long wavelength approach which is similar to lubrication approach, Mishra and Ramachandra Rao [25] have discussed the peristaltic flow in asymmetric channel with asymmetry generated by different amplitudes of the peristaltic waves in addition to different phases. Most of the studies in the literature have been conducted in uniform geometry only whereas it is well known that in most of the practical applications, the flow geometry is found to be non-uniform. Srivastava and Srivastava [26] modeled the peristaltic flow in the vast deferens by assuming it to be a non-uniform diverging channel and a tube. They looked at a more realistic model by evaluating non-Newtonian fluid (Power-law fluid) flow in a non-uniform tube. With increasing interest in particulate suspension flow due to its applications to diverse physical problems, the present study is therefore devoted to study the asymmetric flow of a particulate suspension in a non-uniform channel induced by sinusoidal peristaltic waves. In this study, we, hence, present the generalized model for asymmetric wall – induced peristaltic fluid motion in an infinite two dimensional non-uniform channel which much more accurately simulates intrauterine fluid motion in a sagittal cross-section of the uterus.

As of now, no attempt has been presented for the peristaltic transport of a power law fluid in the tapered asymmetric channel. The purpose of the current study is to discuss such analysis. The governing equations have been solved by using long wavelength and low Reynolds number assumptions. The exact solutions for stream function, longitudinal velocity and pressure gradient have been obtained. The flow quantities are sketched and discussed for the embedded parameters.

## II. MATHEMATICAL FORMULATION

We consider the motion of peristaltic transport of a power law tapered asymmetric channel induced by sinusoidal wave trains propagating at the same speed  $c$  but with different amplitudes and phase differences. The geometry of the wall surface (Figure 1) is described by

$$\begin{aligned}
 H_2(X, t') &= d + m'X + a_2 \sin\left[\frac{2\pi}{\lambda}(X - ct')\right]. & \dots \text{ upper wall,} \\
 H_1(X, t') &= -d - m'X - a_1 \sin\left[\frac{2\pi}{\lambda}(X - ct') + \phi\right]. & \dots \text{ lower wall,}
 \end{aligned} \tag{1}$$

where  $d$  is the half-width of the channel at the inlet of the divergent channel or outlet of convergent channel,  $a_1$  and  $a_2$  are the lower and upper amplitudes of the walls,  $\lambda$  is the wavelength and  $c$  is the phase speed of the wave,  $m' \ll 1$  is a non-uniform parameter of the channel, the phase difference  $\phi$  varies in the range  $0 \leq \phi \leq \pi$ ,  $\phi = 0$  corresponds to symmetric channel with waves out of phase i.e. both walls move towards outward or inward simultaneously.

$$a_1^2 + a_2^2 + 2a_1a_2 \cos(\phi) \leq (2d)^2. \tag{2}$$

### A. The Power-Law Fluid Model

The Ostwald–de Waele power law model as follows [22, 27]

$$\tau = -\left\{ \mu \left| \sqrt{\frac{1}{2}(\Delta : \Delta)} \right|^{n-1} \right\} \Delta, \tag{3}$$

Where  $\tau$  is the stress tensor,  $n$  is the fluid behavior index parameter, and  $\Delta$  is the symmetric part of the velocity gradient tensor.

$$\sqrt{\frac{1}{2}(\Delta : \Delta)} = 2 \left[ \left\{ \left( \frac{\partial U}{\partial X} \right)^2 + \left( \frac{\partial U}{\partial Y} \right)^2 \right\} + \left( \frac{\partial U}{\partial Y} + \frac{\partial V}{\partial X} \right)^2 \right]^{1/2}, \tag{4}$$

The fluid is shear thinning or pseudo plastic fluid if  $n < 1$  and a shear thickening or dilatant fluid if  $n > 1$ . For  $n = 1$ , it becomes Newtonian fluid.

### B. Governing Equations

The equation governing the flow of a Power-law fluid are given by

$$\rho \left( \frac{\partial U}{\partial t'} + U \frac{\partial U}{\partial X} + V \frac{\partial U}{\partial Y} \right) = -\frac{\partial P}{\partial X} + \frac{\partial \tau_{XX}}{\partial X} + \frac{\partial \tau_{YX}}{\partial Y}, \tag{5}$$

$$\rho \left( \frac{\partial V}{\partial t'} + U \frac{\partial V}{\partial X} + V \frac{\partial V}{\partial Y} \right) = -\frac{\partial P}{\partial Y} + \frac{\partial \tau_{XY}}{\partial X} + \frac{\partial \tau_{YY}}{\partial Y}, \tag{6}$$

where

$$\tau_{XX} = |\Phi|^{n-1} 2 \frac{\partial U}{\partial Y}, \quad \tau_{XY} = |\Phi|^{n-1} \left( \frac{\partial U}{\partial Y} + \frac{\partial V}{\partial X} \right), \quad \tau_{YY} = |\Phi|^{n-1} 2 \frac{\partial V}{\partial X}, \tag{7}$$

and  $\rho$  is the density.

To describe the fluid flow in a non-dimensional form, they introduce the following quantities in Eqs. (5-7),

$$x = \frac{X}{\lambda}, \quad y = \frac{Y}{d}, \quad t = \frac{ct'}{\lambda}, \quad u = \frac{U}{c}, \quad v = \frac{V}{\delta c}, \quad \delta = \frac{d}{\lambda}, \quad h_1 = \frac{H_1}{d}, \quad h_2 = \frac{H_2}{d}, \quad p = \frac{d^{n+1}P}{c^n \lambda \mu}. \tag{8}$$

In the Eqs. (5) and (6), we obtain

$$\text{Re} \delta \left( \frac{\partial u}{\partial t} + u \frac{\partial u}{\partial x} + v \frac{\partial u}{\partial y} \right) = -\frac{\partial p}{\partial x} + 2\delta^2 \frac{\partial}{\partial x} \left( \Phi \frac{\partial u}{\partial x} \right) + \frac{\partial}{\partial y} \left\{ \Phi \left( \frac{\partial u}{\partial y} + \delta^2 \frac{\partial v}{\partial x} \right) \right\}, \tag{9}$$

$$\text{Re} \delta^2 \left( \frac{\partial u}{\partial t} + u \frac{\partial v}{\partial x} + v \frac{\partial v}{\partial y} \right) = -\frac{\partial p}{\partial y} + \delta^2 \frac{\partial}{\partial x} \left\{ \Phi \left( \frac{\partial u}{\partial y} + \delta^2 \frac{\partial v}{\partial x} \right) \right\} + 2\delta^2 \frac{\partial}{\partial y} \left( \Phi \frac{\partial v}{\partial y} \right), \tag{10}$$

$$\Phi = \left| 2\delta^2 \left\{ \left( \frac{\partial u}{\partial x} \right)^2 + \left( \frac{\partial v}{\partial y} \right)^2 \right\} + \left( \frac{\partial u}{\partial y} + \delta^2 \frac{\partial v}{\partial x} \right)^2 \right|^{(n-1)/2}. \tag{11}$$

Where  $a(= a_1/d)$ ,  $b(= a_2/d)$ ,  $\delta(= d/\lambda)$  and  $m(= m'\lambda/d)$  is the wave numbers  $\text{Re} (= c^{2-n}d^n\rho/\mu)$  is the Reynolds number for power-law fluid.

Using the long wavelength approximation and neglecting the wave number along with low-Reynolds number, one can find from Eqs. (9-11) that

$$\frac{\partial p}{\partial x} = \frac{\partial}{\partial y} \left( \left| \frac{\partial u}{\partial y} \right|^{n-1} \frac{\partial u}{\partial y} \right), \quad \frac{\partial p}{\partial y} = 0, \quad h_1 \leq y \leq h_2. \tag{12}$$

The corresponding boundary conditions are given by

$$u = 0 \quad \text{on} \quad y = h_1 = -1 - mx - a \sin(2\pi(x-t) + \phi), \tag{13}$$

$$u = 0 \quad \text{on} \quad y = h_2 = 1 + mx + b \sin(2\pi(x-t)). \tag{14}$$

### III. EXACT SOLUTION

It is tough to choose the correct sign for the modulus which appears in the governing Eq. (12). Two appropriate non-unique solutions of Eq. (13-14) satisfying the corresponding boundary conditions along with regularity conditions on the axis are obtained. The longitudinal velocity attains a maximum value on the axis, and the similar regularity condition extends to asymmetric channel geometry.

Hence, we select

$$\frac{\partial u}{\partial y} = 0 \quad \text{for} \quad y = \frac{h_1 + h_2}{2}. \tag{15a}$$

As  $u$  is maximum on the middle line, we have

$$\frac{\partial u}{\partial y} < 0 \quad \text{for} \quad y = \frac{h_1 + h_2}{2} \quad \text{and} \tag{15b}$$

$$\frac{\partial u}{\partial y} > 0 \quad \text{for} \quad y = \frac{h_1 + h_2}{2}. \tag{15c}$$

Solutions of the Eq. (12) using the corresponding the corresponding boundary conditions Eqs. (13-15) are

$$u(y) = \left\{ \begin{array}{l} \left[ \frac{\partial p}{\partial x} \right]^{1/n-1} \left( \frac{\partial p}{\partial x} \right) \left( \frac{n}{n+1} \right) \left[ \left( \frac{h_1+h_2}{2} - y \right)^{1/n+1} - \left( \frac{h_2-h_1}{2} \right)^{1/n+1} \right], \quad h_1 \leq y \leq \frac{h_1+h_2}{2} \\ \left[ \frac{\partial p}{\partial x} \right]^{1/n-1} \left( \frac{\partial p}{\partial x} \right) \left( \frac{n}{n+1} \right) \left[ \left( y - \frac{h_1+h_2}{2} \right)^{1/n+1} - \left( \frac{h_2-h_1}{2} \right)^{1/n+1} \right], \quad \frac{h_1+h_2}{2} \leq y \leq h_2 \end{array} \right. \tag{16}$$

We take the boundary condition for  $\psi$  as

$$\psi = 0 \quad \text{at} \quad y = (h_1 + h_2)/2. \tag{17}$$

Thus the solutions in terms of stream function satisfying the boundary conditions (17) are obtained as



$$\psi(y) = \begin{cases} A \left[ \left( \frac{h_2 - h_1}{2} \right)^{\frac{1}{n}+1} \left( \frac{h_1 + h_2}{2} - y \right) - \frac{n}{2n+1} \left( \frac{h_1 + h_2}{2} - y \right)^{\frac{1}{n}+2} \right], & h_1 \leq y \leq \frac{h_1 + h_2}{2} \\ A \left[ \frac{n}{2n+1} \left( y - \frac{h_1 + h_2}{2} \right)^{\frac{1}{n}+2} + \left( \frac{h_2 - h_1}{2} \right)^{\frac{1}{n}+1} \left( \frac{h_1 + h_2}{2} - y \right) \right], & \frac{h_1 + h_2}{2} \leq y \leq h_2 \end{cases} \quad (18)$$

where  $A = -\left( \frac{1+2n}{2(n+1)} \right) q \left( \frac{2}{h_2 - h_1} \right)^{\frac{1}{n}+2}$ .

When the power-law index  $n=1$  and  $m=0$ , our solutions (18) dilute to a single unique solution given by

$$\psi(y) = \left\{ -\frac{2q}{(h_2 - h_1)^3} \left[ \left( y - \frac{h_1 + h_2}{2} \right)^3 - 3 \left( \frac{h_2 - h_1}{2} \right)^2 \left( y - \frac{h_1 + h_2}{2} \right) \right], \quad h_1 \leq y \leq h_2 \right\} \quad (19)$$

This coincides with that of Mishra and Ramanchandra Rao [25] for peristaltic flow of a Newtonian fluid in an asymmetric channel.

The instantaneous flow rate  $F(x,t)$  is given by

$$F = \int_{h_1}^{h_2} u \, dy = \int_{h_1}^{\frac{h_1+h_2}{2}} u \, dy + \int_{\frac{h_1+h_2}{2}}^{h_2} u \, dy, \quad (20)$$

$$F = \left| \frac{\partial p}{\partial x} \right|^{\frac{1}{n}-1} \frac{\partial p}{\partial x} \left( \frac{h_2 - h_1}{2} \right)^{\frac{1}{n}+2} \left( \frac{-2n}{1+2n} \right). \quad (21)$$

From this, we have

$$\frac{\partial p}{\partial x} = |F|^n \left( \frac{1+2n}{2n} \right)^n \left( \frac{2}{h_2 - h_1} \right)^{1+2n}. \quad (22)$$

The non-dimensional average rise in pressure  $\Delta p$  over one period of wavelength is given by

$$\Delta p = \int_0^1 \int_0^1 \frac{\partial p}{\partial x} \, dx \, dt. \quad (23)$$

#### IV. RESULTS AND DISCUSSION

The reason that the constant value  $F(x,t)$  always produces negative, there shall be no pumping action, and hence, to study the above-obtained results quantitatively, we assume the instantaneous volume rate of the flow  $F(x,t)$ , periodic in  $(x-t)$ , [28, 29] as

$$F(x,t) = \Theta + a \sin 2\pi(x-t) + b \sin[2\pi(x-t) + \phi] \quad (24)$$

Where  $\Theta$  is the time-averaged of the flow flux. The analytical solution of the power-law fluid model in the tapered asymmetric channel is presented. To discuss the effects of various parameters of interest on flow quantities, such as average rise in pressure ( $\Delta p$ ), longitudinal velocity ( $u$ ), and stream function ( $\psi$ ), we have prepared Figs. 2–14. The expression for pressure rise  $\Delta p$  is calculated numerically using mathematics software. The effects of various parameters on the average rise in pressure  $\Delta p$  are shown in Figs. 2-5 for various values of the amplitude of the upper wall ( $b$ ), non-uniform parameter ( $m$ ), power law index ( $n$ ) and phase difference ( $\phi$ ). Figs. 2-5 are alienated four parts so that the upper right-hand quadrant denotes the region of peristaltic pumping where  $Q > 0$  (positive pumping) and  $\Delta p > 0$  (adverse pressure gradient). The lower right-hand quadrant denotes the region of augmented pumping  $Q > 0$  (positive pumping) and  $\Delta p < 0$  (favorable pressure gradient), and the upper left-hand quadrant denotes the region of retrograde pumping (or backward pumping) where  $Q < 0$  (negative pumping) and  $\Delta p > 0$  (adverse pressure gradient) wherein the flows are opposite to the direction of the peristaltic motion. It is evident from figures that there is non-linear relations between  $\Delta p$  and  $Q$  for all  $n > 1$  and  $n < 1$  but not  $n = 1$ .

It is considered that from Fig. 2 that the retrograde ( $\Delta p > 0, Q < 0$ ) and peristaltic pumping ( $\Delta p > 0, Q > 0$ ) regions and the pumping rate increase with an increase in the amplitudes of the upper wall ( $b$ ), while in the copumping ( $\Delta p < 0, Q > 0$ ) region, the behavior is quite opposite. Fig. 3 shows the variation of average rise in pressure with the mean flow rate for different values of  $m$ . It shows that the average rise in pressure decreases with an increase in the mean flow rate. We also notice that for the fixed value of  $Q$ , average rise in pressure decreases when  $m$  increases. The variation of average rise in pressure with the mean flow rate for different values of  $n$  is shown in Fig. 4. From this figure, It is observed that  $\Delta p$  increases with an increase of power-law behaviour index  $n$ , indicating that pumping increases as the fluid character changes from shear thinning ( $n < 1$ ) to Newtonian ( $n = 1$ ) and to shear thickening ( $n > 1$ ). Fig. 5 gives the effects of phase difference  $\phi$  on  $\Delta p$ . It is clear that an increase in  $\phi$  results in a decrease of the peristaltic pumping rate, free pumping ( $\Delta p = 0$ ) and the adverse pressure rise ( $\Delta p > 0$ ).

The expression for longitudinal velocity in term of  $y$  has been given in Eq. (16). Figs. 6-9 are plotted to study the effects of various physical parameters on the velocity distribution in the tapered asymmetric channel. Fig. 6 is drawn to study the effect of  $a$  on the longitudinal velocity. It reveals that the longitudinal velocity profiles are parabolic and it increases with increasing  $a$ . The effect of the non-uniform parameter  $m$  on  $u$  is demonstrated in Fig. 7. It is observed that the longitudinal velocity  $u$  increases at close to the walls while the reverse situation is observed in the core part of the trapped channel. Fig. 8 reveals that the longitudinal velocity near the channel walls is not similar in view of the power-law index  $n$ . The longitudinal velocity increases by increasing  $n$  in the hub of the channel. Fig. 9 displays the effects of mean flow rate ( $Q$ ) on the longitudinal velocity distribution. It is found that the longitudinal velocity increases as  $Q$  increases.

Another inspiring phenomena of peristalsis is trapping, the expression of an internally circulating bolus of fluid which moves along with the wave. Fig.10 shows that by increasing in  $b$ , the trapping bolus increases in the upper and lower parts of the channel. Fig. 11 illustrates that the effects of non-uniform parameter  $m$  on the trapping. It is concluded that the size of the bolus increases with an increase in  $m$ . The sound effect of the power-law index  $n$  on the trapping is shown in Fig. 12. It is examined that the size of the channel increases with an increase in  $n$ . The effects of the phase difference  $\phi$  on trapping we have prepared Fig.13. We note that the increase in the phase difference decreases the trapped bolus on the lower and upper part of the tapered asymmetric channel. Fig. 14 viewed that the size of the trapping bolus increases with an increase in  $Q$ .

### V. CONCLUSIONS

A mathematical model to study the peristaltic transport of the power-law fluid in the tapered asymmetric channel is investigated. The problem is studied under the assumption of long-wavelength and low-Reynolds number approximations. The results are discussed through graphs. We conclude the following observations:

- 1) For non-Newtonian fluid, the average rise in pressure is larger than Newtonian fluid.
- 2) It is observed that for  $n \neq 1$ , the curves of the  $\Delta p$  versus  $Q$  are not linear.
- 3) The increases in power law index enhance the area of trapped bolus size.
- 4) The size of trapped bolus increases with increasing  $b$  and  $Q$  while decreases with increasing  $\phi$ .
- 5) The results obtained by us agree with those obtained by Mishra and Rao [25] when  $m = 0$  and  $n = 1$ .

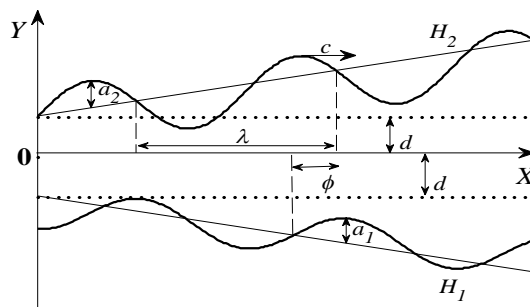


Fig. 1 Schematic diagram of tapered asymmetric channel

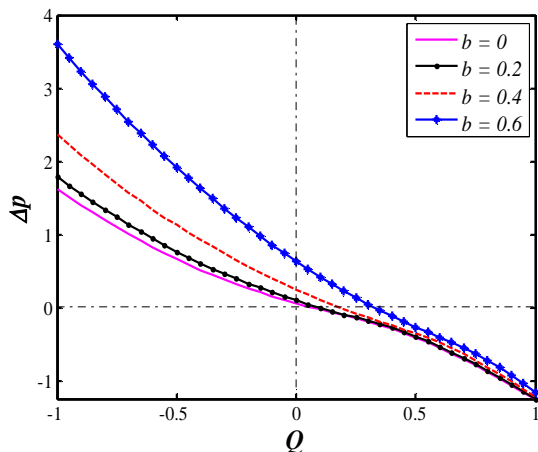


Fig. 2 The pressure rise versus flow rate for  $a = 0.3; m = 0.1; \phi = \pi/2$  and  $n = 1.5$ .

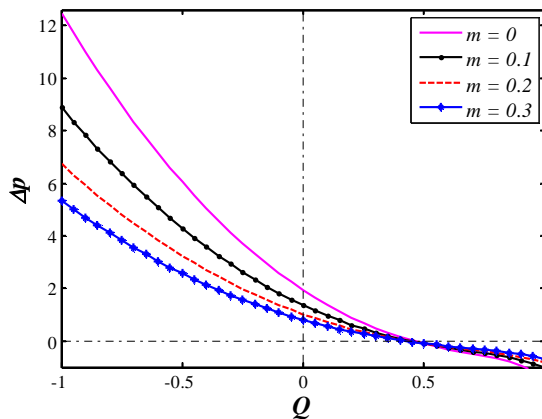


Fig. 3 The pressure rise versus flow rate for  $a = 0.6; b = 0.5; \phi = \pi/2$  and  $n = 2$ .

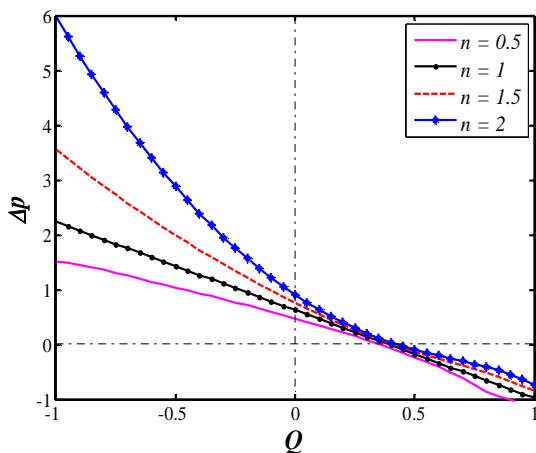


Fig. 4 The pressure rise versus flow rate for  $a = 0.4; b = 0.5; m = 0.25$ ; and  $\phi = \pi/3$ .

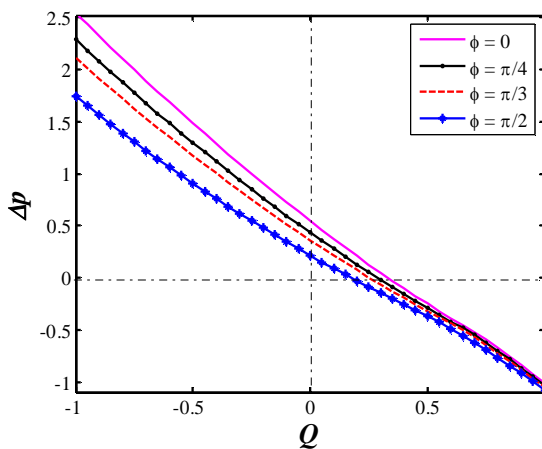


Fig. 5 The pressure rise versus flow rate for  $a = 0.4; b = 0.3; m = 0.2$  and  $n = 1.25$ .

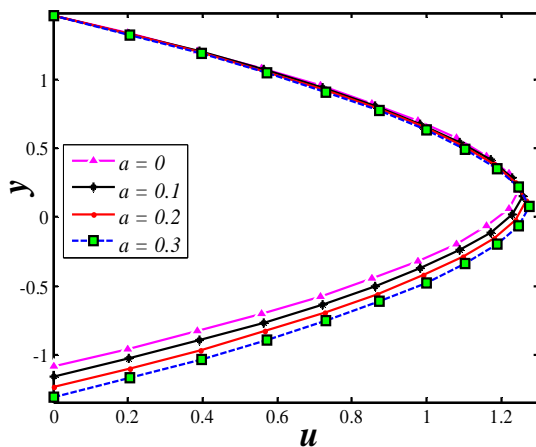


Fig. 6 The effect of  $a$  on velocity profiles at  $b = 0.4; m = 0.2; n = 1.5; Q = 1.6; \phi = \pi/3; x = 0.4$  and  $t = 0.2$ .

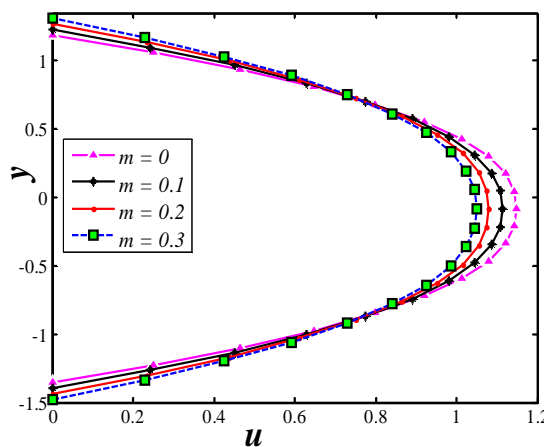


Fig. 7 The effect of  $m$  on velocity profiles at  $a = 0.4; b = 0.2; n = 0.75; Q = 1.5; \phi = \pi/4; x = 0.4$  and  $t = 0.2$ .

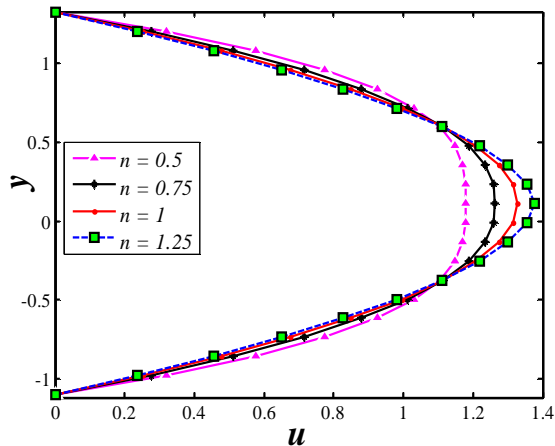


Fig. 8 The effect of  $n$  on velocity profiles at  $a = 0.2; b = 0.3; m = 0.1; Q = 1.8; \phi = \pi/2; x = 0.4$  and  $t = 0.2$ .

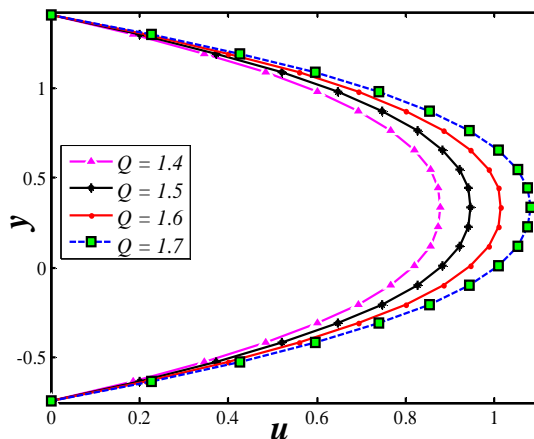
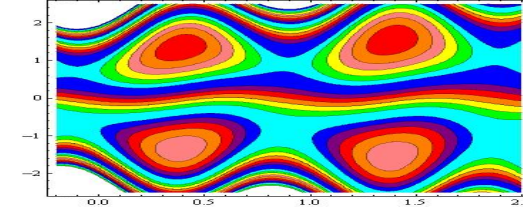
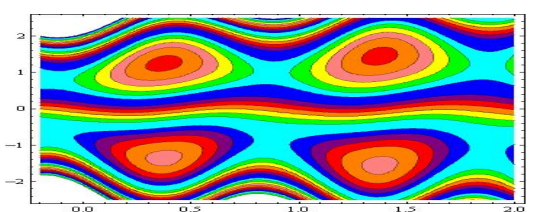
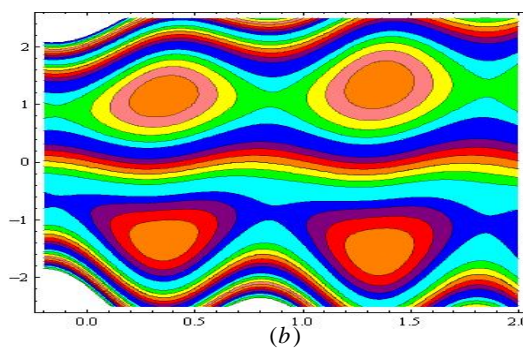
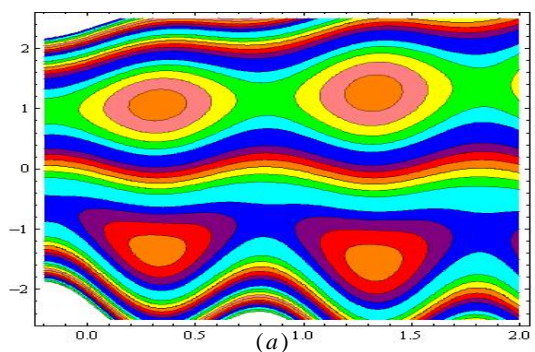


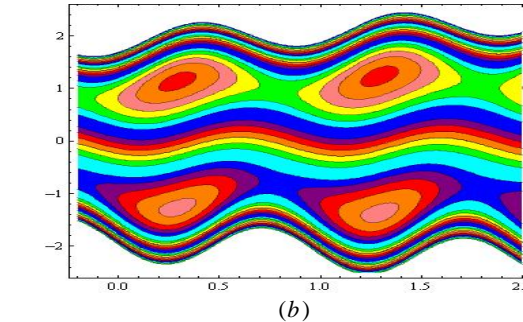
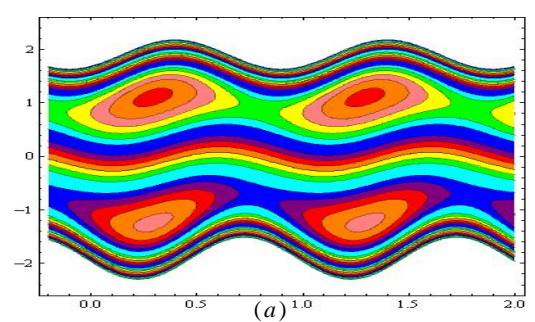
Fig. 9 The effect of  $n$  on velocity profiles at  $a = 0.4; b = 0.3; m = 0.3; n = 0.8; \phi = \pi; x = 0.4$  and  $t = 0.2$ .



(c)

(d)

Fig. 10 Plot showing streamlines for four different parameter  $b$  values  $b = 0$  (panel (a)),  $b = 0.1$  (panel (b)),  $b = 0.2$  (panel (c)) and  $b = 0.3$ . (panel (d)). The other parameters chosen are  $a = 0.3, m = 0.2, \phi = \pi/4, n = 1.75, Q = 1.4, t = 0.2$ .



(a)

(b)



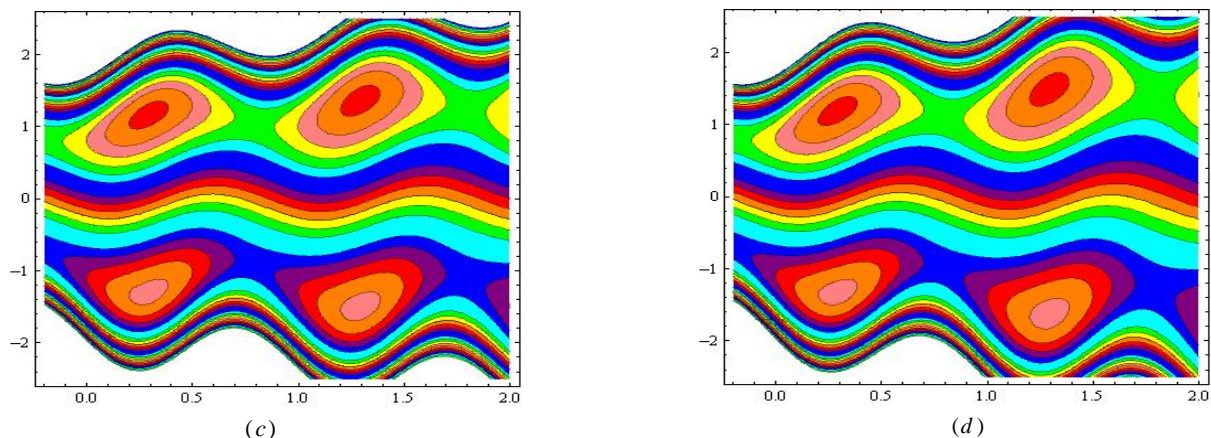


Fig. 11 Plot showing streamlines for four different parameter  $m$  values  $m = 0$  (panel (a)),  $m = 0.1$  (panel (b)),  $m = 0.2$  (panel (c)) and  $m = 0.3$ . (panel (d)). The other parameters chosen are  $a = 0.3$ ,  $b = 0.2$ ,  $\phi = \pi / 2$ ,  $n = 0.5$ ,  $Q = 1.5$ ,  $t = 0.2$ .

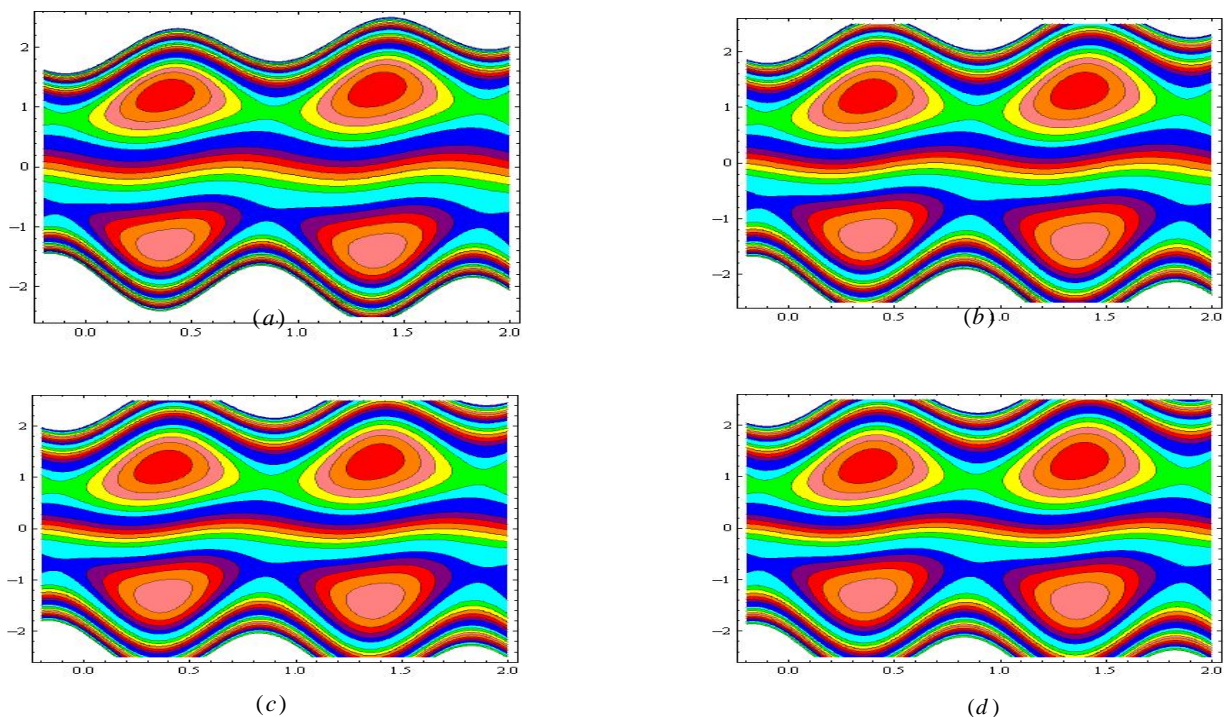
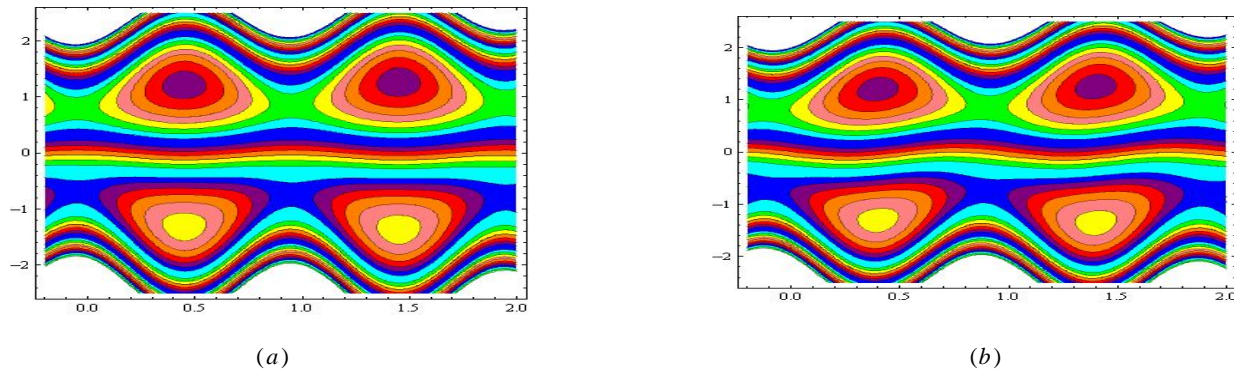


Fig. 12 Plot showing streamlines for four different parameter  $n$  values  $n = 0.5$  (panel (a)),  $n = 1$  (panel (b)),  $n = 1.5$  (panel (c)) and  $n = 2$  (panel (d)). The other parameters chosen are  $a = 0.3$ ,  $b = 0.2$ ,  $\phi = \pi / 4$ ,  $m = 0.1$ ,  $Q = 1.5$ ,  $t = 0.2$ .





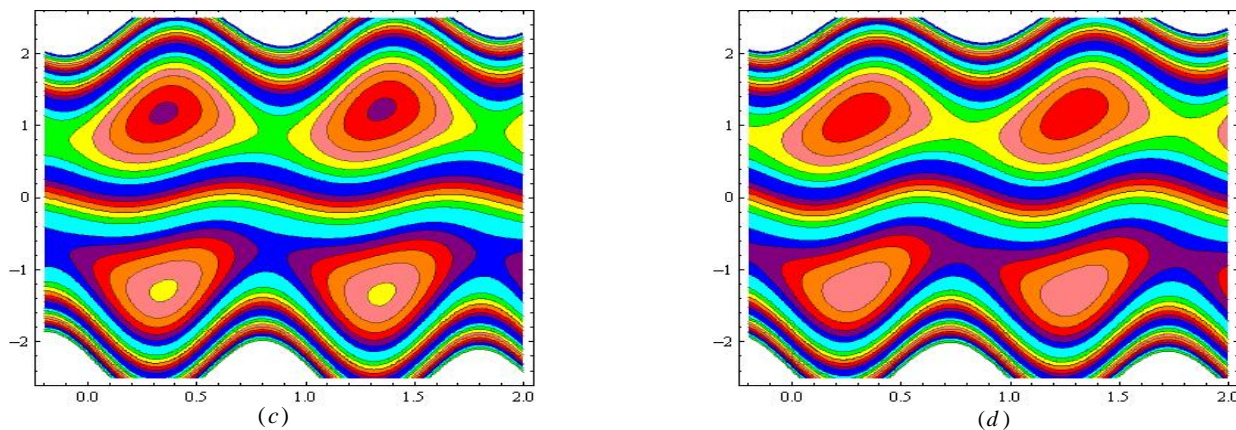


Fig. 13 Plot showing streamlines for four different parameter  $\phi$  values  $\phi = 0$  (panel (a)),  $\phi = \pi/6$  (panel (b)),  $\phi = \pi/3$  (panel (c)) and  $\pi/2$  (panel (d)). The other parameters chosen are  $a = 0.3$ ,  $b = 0.2$ ,  $n = 2$ ,  $m = 0.05$ ,  $Q = 1.6$ ,  $t = 0.2$ .

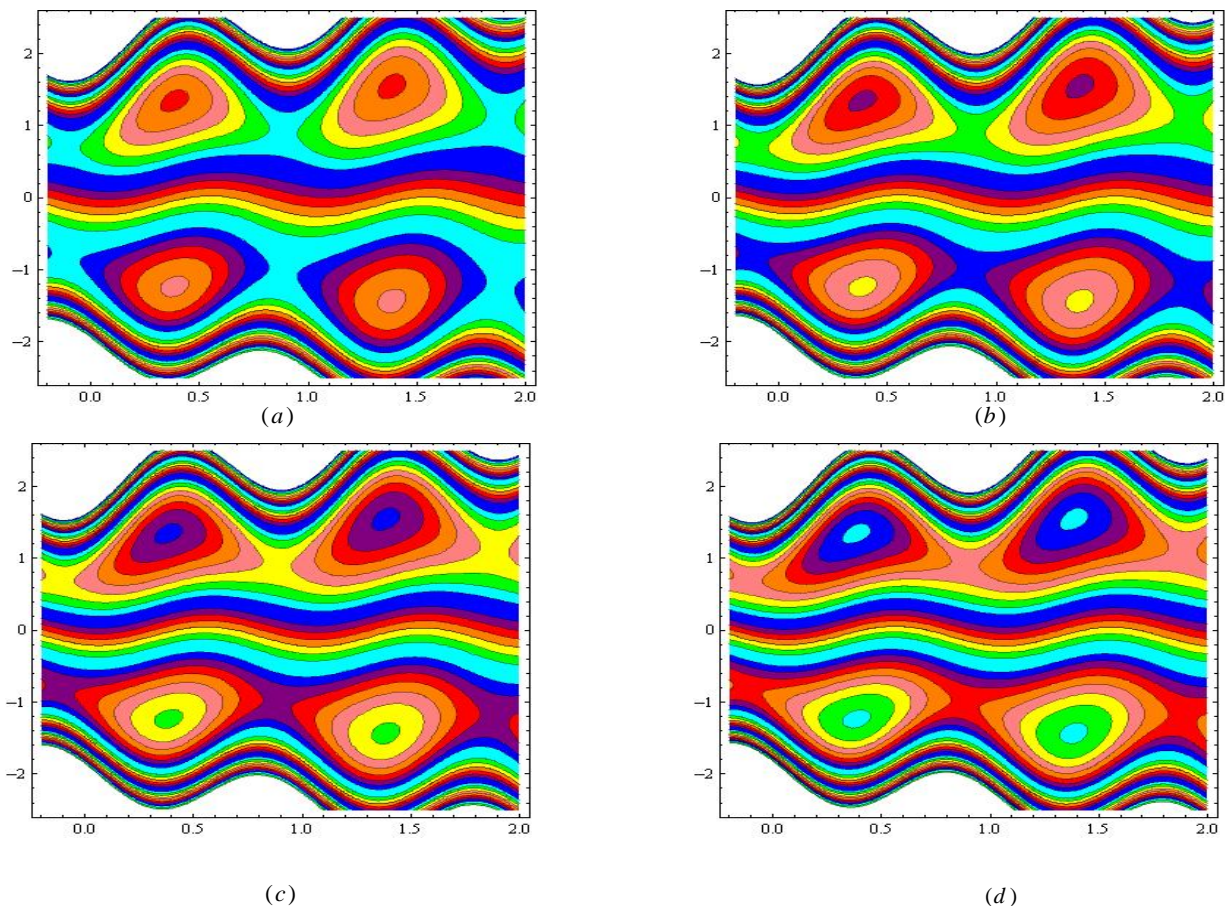


Fig. 14 Plot showing streamlines for four different parameter  $Q$  values  $Q = 1.4$  (panel (a)),  $Q = 1.6$  (panel (b)),  $Q = 1.8$  (panel (c)) and  $Q = 2$  (panel (d)). The other parameters chosen are  $a = 0.3$ ,  $b = 0.2$ ,  $n = 2$ ,  $m = 0.05$ ,  $Q = 1.6$ ,  $t = 0.2$ .

#### REFERENCES

- [1] T.W. Latham, Fluid motion in a peristaltic pump. Cambridge: MS Thesis, MIT, 1966.
- [2] Y.C. Fung, C.S. Yih, Peristaltic transport, J. App. Mech. 35 (1968) 669 - 675.

- [3] A.H. Shapiro, M.Y. Jaffrin, S.L. Weinberg, Peristaltic pumping with long wavelengths at low Reynolds number, *J. Fluid Mech.* 37 (1969) 799 - 825.
- [4] M.Y. Jaffrin, A.H. Shapiro, Peristaltic pumping, *Annual Review of Fluid Mechanics* 3 (1971) 13 - 37.
- [5] J.C. Misra, S.K. Pandey, Peristaltic flow of a multilayered power-law fluid through a cylindrical tube, *Int. J. Eng. Sci.* 39 (2001) 387 - 402.
- [6] K. Vajravelu, S. Sreenadh, B.R. Babu, Peristaltic transport of a Herschel-Buckley fluid in an inclined tube, *Int. J. Non-Linear Mech.* 40 (2005) 83 - 90.
- [7] K. Vajravelu, G. Radhakrishnamacharya , V. Radhakrishnamurty, Peristaltic flow and heat transfer in a vertical porous annulus with long wave approximation, *Int. J. Non-Linear Mech.* 42 (2007) 754.
- [8] M. Kothandapani, S. Srinivas, Non-linear peristaltic transport of a Newtonian fluid in an asymmetric channel through a porous medium, *Phys. Lett. A* 372 (2008) 1265 – 1276.
- [9] M. Kothandapani, S. Srinivas, On the influence of wall properties in the MHD peristaltic transport with heat transfer and porous medium, *Phys. Lett. A* 372 (2008) 4586–4591.
- [10] C. Dhanapal, J. Kamalakkannan, J. Prakash, J. Kothandapani, Analysis of peristaltic motion of a nanofluid with wall shear stress, microrotation and thermal radiation effects, *Appl. Bionics Biomech.* 412374 (2016) 412374.
- [11] J. Prakash, E.P. Siva, D. Tripathi, M. Kothandapani, Nanofluids flow driven by peristaltic pumping in occurrence of magnetohydrodynamics and thermal radiation, *Mater. Sci. Semicond. Process.* 100 (2019) 290-300.
- [12] R. Vijayaragavan, P. Tamizharasi, A. Magesh, Brownian motion and thermoporesis effects of nanofluid flow through the peristaltic mechanism in a vertical channel, *J. Porous Media*, 25(6) (2022) 65–81.
- [13] A. Ramachandra Rao, M. Mishra, Peristaltic transport of a power-law fluid in a porous tube, *Int. J. Non-Linear Mech.* 121 (2004) 163 - 174.
- [14] T. Hayat, F.M. Mahomed, S. Asghar, Peristaltic flow of a magnetohydrodynamic Johnson-Segalman fluid, *Nonlinear Dynamics* 40 (2005) 375 - 385.
- [15] M.V. Subba Reddy, A. Ramachandra Rao, S. Sreenadh, Peristaltic motion of a power-law fluid in an asymmetric channel, *Int. J. Non-Linear Mech.* 42 (2007) 1153 - 1161.
- [16] M. Kothandapani, J. Prakash, Effects of thermal radiation parameter and magnetic field on the peristaltic motion of Williamson nanofluids in a tapered asymmetric channel, *Int. J. Heat Mass Transf.* 81 (2015) 234-245.
- [17] A. Magesh, M. Kothandapani, V. Pushparaj, Electro-osmotic flow of Jeffery fluid in an asymmetric micro-channel under the effect of magnetic field, *J. Phys. Conf. Ser.* 1850 (2021) 012102.
- [18] K.K. Raju, R. Devanathan, Peristaltic motion of a non-Newtonian fluid, *Rheol. Acta.* 11 (1972) 170-178.
- [19] G. Radhakrishnamacharay, Long wave length approximation to peristaltic motion of a power law fluid, *Rheol. Acta* 21 (1982) 30-35.
- [20] J.B. Shukla, S.P. Gupta, Peristaltic transport of a power-law fluid with variable consistency, *ASME J. Biomech. Eng.* 104 (1982) 182-186.
- [21] L.M. Srivastava, V.P. Srivastava, Peristaltic transport of blood: Casson model – II, *J.Biomech.* 17 (1984) 821-829.
- [22] O. Eytan, D. Elad, Analysis of intra-uterine motion induced by uterine contractions, *Bull. Math. Biol.* 61 (1999) 221–238.
- [23] O. Eytan, A.J. Jaffa, D. Elad, Peristaltic flow in a tapered channel: application to embryo transport within the uterine cavity, *Med. Eng. Phys.* 23 (2001) 473–482.
- [24] M.V. Subba Reddy, A. Ramachandra Rao, S. Sreenadh, Peristaltic motion of a power law fluid in an asymmetric channel, *Int. J. Non-Linear Mech.* 42 (2007) 1153 – 1161.
- [25] M. Mishra, A. Ramachandra Rao, Peristaltic transport of a Newtonian fluid in an asymmetric channel, *Z. Angew. Math. Phys.* 54 (2003) 532–550.
- [26] L.M. Srivastava, V.P. Srivastava, Peristaltic transport of a non-Newtonian fluid (application to the vas deferens at small intestine), *Annals of Biomedical Eng.* 13 (1985) 137–153.
- [27] R.B. Bird, W.E. Stewart, E.N. Lightfoot, *Transport Phenomena*, Wiley, Singapore, 1960.
- [28] L.M. Srivastava , V.P. Srivastava, S.N. Sinha, Peristaltic Transport of a Physiological Fluid: Part I. Flow in Non–Uniform Geometry, *Biorheol.* 20 (1983) 153–166.
- [29] L.M. Srivastava, V.P. Srivastava, Peristaltic Transport of a Power-Law Fluid: Application to the Ductus Efferentes of the Reproductive Tract, *Rheol. Acta* 27 (1988) 428–433.





10.22214/IJRASET



45.98



IMPACT FACTOR:  
7.129



IMPACT FACTOR:  
7.429



# INTERNATIONAL JOURNAL FOR RESEARCH

IN APPLIED SCIENCE & ENGINEERING TECHNOLOGY

Call : 08813907089  (24\*7 Support on Whatsapp)